ELSEVIER

Sensors and Actuators A 102 (2003) 279–285

SENSORS AND ACTUATORS A PHYSICAL

www.elsevier.com/locate/sna

Materials selection for microfabricated electrostatic actuators

V.T. Srikar*, S.M. Spearing

Department of Aeronautics and Astronautics, Massachusetts Institute of Technology, Room 33-318, 77 Massachusetts Avenue, Cambridge, MA 02139, USA

Received 22 June 2002; received in revised form 24 September 2002; accepted 3 October 2002

Abstract

Microfabricated electrostatic actuators are employed in a wide variety of microelectromechanical systems (MEMS) for applications ranging from relays and switches to valves and displays. The rapid expansion of the set of materials available to MEMS designers motivates the need for a systematic and rational approach toward the selection of materials for electrostatic actuators. We apply the Ashby methodology to accomplish such a selection. The primary performance and reliability metrics considered are the actuation voltage, speed of actuation, stroke (or displacement), actuation force, stored energy, electrical resistivity, mechanical quality factor, and resistance to fracture, fatigue, shock, and stiction. The materials properties governing these parameters are the Young's modulus, density, fracture strength, intrinsic residual stress, resistivity, and intrinsic material damping. Materials indices are formulated by appropriate combination of these properties and a graphical procedure for materials selection is presented. Our analysis suggests that diamond, alumina, silicon carbide, silicon nitride, and silicon are excellent candidates for high-speed, high-force actuators; polymers for large-displacement, low actuation-voltage devices; and aluminum for low-electrical resistivity, low actuation-voltage and high-speed actuators. The properties of composite actuator structures are briefly discussed.

Keywords: Design; Materials selection; Electrostatic actuators; Actuation voltage; Actuation speed; Reliability

1. Introduction

Electrostatic forces are seldom considered for the actuation of macroscale structures [1]. In contrast, electrostatic actuators are widely employed as prime movers in a variety of microelectromechanical systems (MEMS) [2–4]. The applications for such devices include electromechanical switches and relays [5], optical switches [6], displays [2], valves [7], flow control actuators [8], microscale mechanical testing instruments and structures [9–13], and tunable vertical cavity lasers [14]. As a consequence of their popularity and utility, many aspects of the design of electrostatic actuators—the nature of the pull-in electromechanical instability [11,15], characteristics of the displacement during actuation [16–19], shape and location of electrodes [20–23], speed-energy tradeoffs [24,25], optimization of the actuation force [26,27], dynamics of actuation [28–30], the effects of residual stresses and support compliance [31], and reliability [32]—have been studied in detail.

An important aspect of design that has received little attention is the selection of materials for electrostatic actuators [33]. Processing considerations have made silicon a popular choice for actuator material, but recent advances in micromachining techniques now enable the integration of a number of different metals, alloys, ceramics, glasses, and polymers into MEMS [34]. Examples of materials used to fabricate electrostatic actuators include silicon dioxide [35], aluminum [5], nickel [36], diamond [37,38], silicon carbide [39], Ta−Si−N [7], and parylene [8]. As the MEMS materials set continues to expand, there is a clear need for a rational and systematic approach toward the selection of materials in micromechanical design.

An approach to materials selection in the design of macroscale structures has been suggested by Ashby [40,41]. We have recently extended this approach to MEMS design [42]. In this paper, these techniques are applied to the selection of materials for electrostatic actuators. Section 2 contains a brief description of the important performance metrics of electrostatic actuators based on a lumped-parameter representation. The materials properties governing these metrics are discussed in Section 3, leading to the formulation of *materials indices*. Materials selection graphs, which are plots with axes

* Corresponding author. Tel.: +1-617-452-2869; fax: +1-617-258-6666.
E-mail addresses: srikar@mtl.mit.edu, vts@alum.mit.edu (V.T. Srikar), spearing@mit.edu (S.M. Spearing).

0924-4247/03/$ – see front matter
PII: S0924-4247(02)00393-X

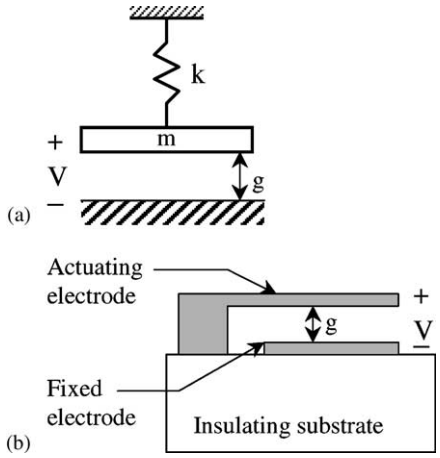

Fig. 1. (a) Lumped-parameter representation of an electrostatic actuator. (b) Schematic cross-section of a beam electrostatic actuator.

corresponding to different materials indices, are presented in Section 4. Many electrostatic actuators are laminated composite structures; the properties of such structures are briefly discussed in Section 5.

2. Performance indices

A good first-order representation of a voltage-controlled electrostatic actuator is the lumped-parameter model shown in Fig. 1(a) [2]. When a potential difference is maintained between the plate (of mass m) and the fixed ground electrode, the magnitude of the electrostatic force (F_e) acting on the plate is given by [2]

$$F_e = -\frac{\varepsilon A V^2}{2g^2} \tag{1}$$

where ε is the permittivity of the air in the gap, A the area of the plate, V the applied voltage, and g is the size of the gap between the plate and the electrode. The mechanical force (F_M) exerted by the spring on the plate is given by [2]

$$F_M = k\delta = k(g_0 - g) \tag{2}$$

where k is the stiffness of the spring, g_0 the initial (unactuated) gap size, and δ is the displacement of the actuator. The plate is in equilibrium when the two forces are equal. The actuation voltage (V) is, hence, given by [2]

$$V = \sqrt{\frac{2kg^2(g_0 - g)}{\varepsilon A}} \tag{3}$$

When the gap is reduced to two-thirds the initial size, i.e. $g = 2g_0/3$, the stability of the equilibrium is lost, and the plate collapses (or *pulls-in*) onto the ground electrode [2]. From Eq. (3), the collapsing voltage (or pull-in voltage, V_{PI}) is given by

$$V_{PI} = \sqrt{\frac{8kg_0^3}{27\varepsilon A}} \tag{4}$$

The speed of actuation (s) is, to first-order, directly proportional to the natural frequency of vibration (f) of the spring–mass system [29]. This can be expressed as

$$s \propto f = \frac{1}{2\pi}\sqrt{\frac{k}{m}} \tag{5}$$

The mechanical quality factor (Q) is a measure of the damping of the actuator. Electrostatic actuators operated under ambient conditions exhibit Q-values typically in the range 10–200; air- and squeezed-film damping are typically the dominant dissipative mechanisms. (The speed of actuation of heavily damped actuators is expected to be independent of the mechanical properties of the actuator material [29].)

The electrostatic energy ($U_{Electrostatic}$) stored in the actuator is given by [2]

$$U_{Electrostatic} = \frac{\varepsilon A V^2}{2g} \tag{6}$$

and the elastic energy ($U_{Elastic}$) stored in the spring is given by [2]

$$U_{Elastic} = \tfrac{1}{2}kg^2 \tag{7}$$

The stiffer the spring, the higher the energy stored in the actuator.

3. Materials indices

The next step in the process of materials selection is to express explicitly the various performance metrics as functions of the applied load, structural geometry, and materials properties. We illustrate this procedure using a prismatic beam (of thickness h, width b, and length L) as the actuator structure of interest (Fig. 1(b)); extensions to plates, membranes, and other structures could be achieved using an analogous calculation. In what follows, we discuss the various properties of the beam sequentially. Failure due to fatigue, shock, and stiction is also discussed.

3.1. Stiffness

The stiffness of the beam (k_{beam}) is given by [40]

$$k_{beam} = \frac{F}{\delta} = \frac{C_1 EI}{L^3}, \qquad M_1 = E \tag{8}$$

where F is the applied force, δ the displacement, C_1 a constant (dependent on the details of the loading and boundary conditions), E the Young's modulus, and I is the moment of inertia of the beam. It is clear that the only materials property governing the stiffness is the Young's modulus. This is identified as a *materials index*, M_1. For arbitrary beam geometry, loading, and boundary conditions, the stiffness can be optimized (maximized or minimized) by choosing materials with optimal values of M_1. (Since the actuation voltage is proportional to the square root of the stiffness, it is convenient to define $M_2 = \sqrt{E}$.)

3.2. Frequency

The frequency of flexural vibrations of the beam can be expressed as [40]

$$f = \frac{C_2}{2\pi}\sqrt{\frac{Eh^2}{12\rho L^4}}, \qquad M_3 = \sqrt{\frac{E}{\rho}} \tag{9}$$

where C_2 is a constant and ρ is the density. The materials index, M_3 is also the speed of propagation of longitudinal waves in the material. Materials with high wave-speeds are, therefore, good candidates for high-speed actuators.

3.3. Energy, force and stroke

From Eqs. (1), (3), (7) and (8), it follows that the actuation force and stored energy are directly proportional to the stiffness. Therefore, the higher the value of M_1, the higher the actuation force and energy. Conversely, the higher the stiffness, the lower the displacement for a given force. The maximum displacement (or stroke) of the actuator is limited by the failure strength (σ_f) of the material (yield and fracture strength for ductile and brittle materials, respectively). The displacement of the beam can be related to the maximum tensile stress (σ_0) by the expression [40]

$$\delta = \frac{2L^2}{3h}\frac{\sigma_0}{E}, \qquad M_4 = \frac{\sigma_f}{E} \tag{10}$$

Materials with large values of M_4 are good candidates for high-stroke actuators. It is important to note that the fracture strength is a stochastic variable and is sensitively dependent on the processing conditions.

3.4. Electrical resistivity

In some applications, for example, in low-loss microwave switches [5], it is desirable for the actuating electrode to have a low electrical resistivity (ρ_e). Therefore,

$$M_5 = \rho_e \tag{11}$$

3.5. Residual stress

Micromachined structures fabricated using deposited thin films are invariably in a state of residual stress. These stresses can influence the actuation voltage, speed of actuation, and reliability of electrostatic actuators [2]. The magnitude of the intrinsic residual stress in a micromachined structure is sensitively dependent not only on the processing technique used, but also on the details of the processing parameters (argon pressure in sputtering, temperature of deposition in chemical vapor-deposition, etc.). For the purposes of materials selection, it is important to note that, for many metals and ceramics, the residual stress can be tuned over a wide range of several hundred megapascals by appropriate choice of process parameters [42].

3.6. Mechanical quality factor (Q)

The quality factor (Q) of a resonator is proportional to the ratio of the maximum potential energy to the total energy dissipated per cycle of vibration. The quality factors of microdevices operated under ambient conditions are, to first-order, independent of materials properties. However, in vacuum-operated devices with suitably engineered support structures, the intrinsic material damping becomes the dominant mechanism of dissipation [43,44]. As initial design values for intrinsically limited Q, we suggest the following bounds for various classes of materials [42]:

$$\begin{cases} 10^4 < Q < 10^7 & \text{(ceramics)} \\ 10^3 < Q < 10^5 & \text{(metals)} \\ Q < 10^2 & \text{(polymers)} \end{cases} \tag{12}$$

3.7. Stiction

Stiction refers to adhesion-induced immobilization of mechanical elements. Such immobilization can occur when a collapsing force (due to capillarity, shock, actuation, etc.) brings adjacent structures into contact and solid–solid adhesion prevents separation. From a materials viewpoint, an approach to reduce stiction is by the use of low-energy self-assembled coatings (see, for example, [45]). These coatings are sufficiently thin (approximately a few nanonmeters) as to have negligible effect on the mechanical properties of the structure.

3.8. Fatigue resistance

Structures that are subjected to repeated stress cycles may fail at stresses significantly lower than the fracture strength. Fatigue-induced damage of MEMS structures is currently a topic of active research [46]; the fatigue life of a device is typically evaluated experimentally. Anecdotal evidence suggests that the resistance to fatigue increases with decreasing length scale. Lifetimes in excess of 10^9 cycles have been reported in polysilicon [10], aluminum [5], silicon dioxide [35], and nickel [36] microfabricated structures.

3.9. Shock reliability

Many electrostatically actuated devices can be subjected to shock loads during fabrication, deployment, or operation. The common modes of failure in shock environments include delamination, fracture, and stiction [32]. The selection of materials for improved shock reliability has previously been discussed [42].

4. Materials selection charts

The optimal values of the performance metrics are strongly application-dependent. For instance, a low actuation voltage

is desirable in many applications including displays and switches, whereas a high actuation voltage is essential in applications requiring large forces. Similarly, a high mechanical quality factor (Q) improves the performance of sensors, whereas a low Q leads to improved dynamic behavior in displays [2] and switches [30]. Moreover, some performance metrics can impose conflicting demands on the materials indices, a common example being the combination of high speed (i.e. high $\sqrt{E/\rho}$) and low actuation voltage (i.e. low $\sqrt{E}$).

A convenient method of comparing and selecting materials based on the relative values of their materials indices is through the use of materials selection charts [40]. These are graphs with axes corresponding to different materials indices; the scale on each axis is chosen to accommodate all materials of interest. A common feature of such charts is that, in general, materials of a class (i.e. metals, ceramics, polymers) tend to cluster together. These charts can be used not only to identify optimal materials choices for each performance metric, but also to identify optimal trade-offs when the metrics are in conflict.

Fig. 2 is a materials selection chart for existing microfabricated materials with axes of $\sqrt{E}$ and $\sqrt{E/\rho}$. It is clear that the materials that maximize speed also require high actuation voltages, and vice versa. A trade-off line can be identified as shown on the figure [41]. Materials that lie on, or close to, this line are the best candidates for actuators; the choice depends on the relative importance of speed and actuation voltage. Candidate materials for actuators requiring a high speed of operation are diamond, silicon carbide, alumina, silicon nitride, and silicon. Similarly, polymers, lead and tin are the materials of choice when the actuation voltage is to be minimized, although linearity and hysterisis in mechanical response may be issues. For combinations of modestly high speeds and low actuation voltages, Fig. 2 suggests that silicon dioxide, quartz, aluminum, and titanium are good candidates. As the MEMS materials set continues to expand, the coordinates of new materials can be located on charts such as these to evaluate their utility for various applications.

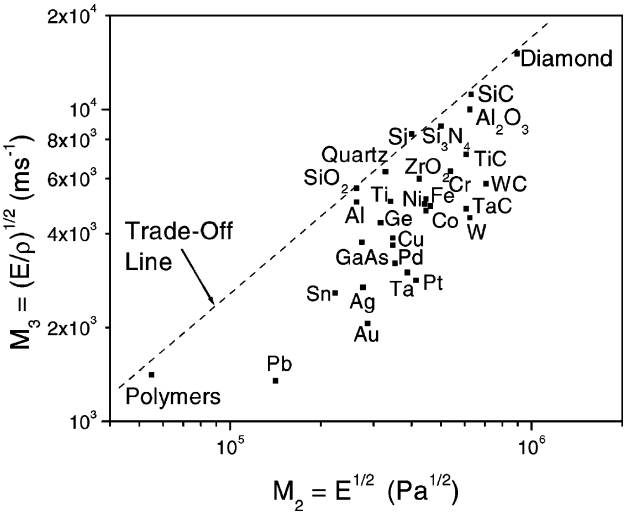

Fig. 2. A materials selection chart with the wave-speed $\sqrt{E/\rho}$ plotted against the square root of the Young's modulus.

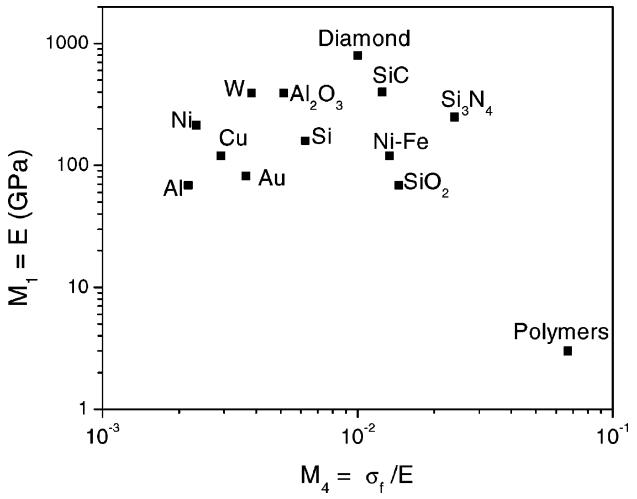

Fig. 3. A materials selection chart with the Young's modulus (E) plotted against the ratio of the fracture strength (σ_f) to the Young's modulus.

Next, we address the force and stroke of the actuator. Fig. 3 is a materials selection chart with axes of E and (σ_f/E). From Figs. 2 and 3, materials for large-force actuators are diamond, alumina, silicon carbide, titanium carbide, tantalum carbide, tungsten carbide, and tungsten. Polymers are very attractive candidates for large-stroke actuators. As mentioned previously, the fracture strength depends strongly on the processing conditions. The nominal values shown in Fig. 3 are intended to guide only the initial choice of materials. Experimental determination of fracture strengths is usually required to narrow the choice of materials.

As mentioned earlier, a low value of the electrical resistivity is required in some applications. Figs. 4 and 5 are materials selection charts with the electrical resistivity

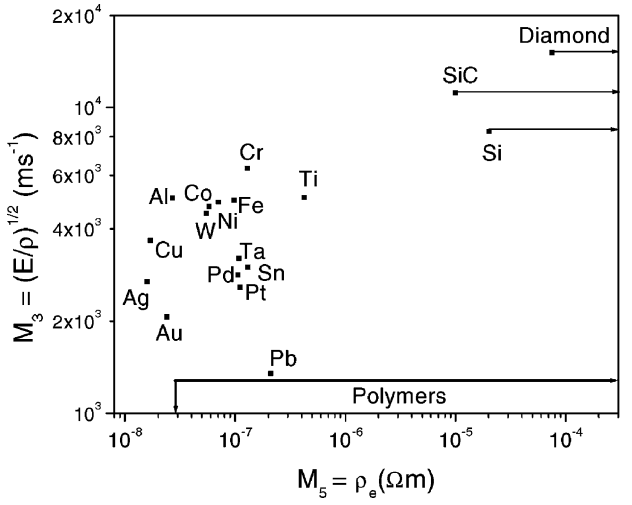

Fig. 4. A materials selection chart with the wave-speed $\sqrt{E/\rho}$ plotted against the electrical resistivity.

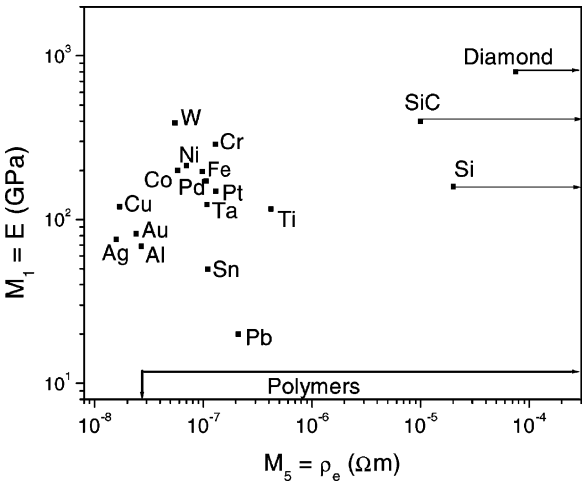

Fig. 5. A materials selection chart with the Young's modulus (E) plotted against the electrical resistivity.

(at 300 K) plotted against the wave-speed and the Young's modulus, respectively. The large range of resistivity values indicated for silicon, silicon carbide, diamond, and polymers is indicative of their sensitivity to doping. The Young's modulus and density are relatively weak functions of the doping concentration and only the nominal values of these properties are shown in Figs. 4 and 5. Of the materials that exhibit the lowest resistivities (silver, copper, gold and aluminum), aluminum has the best combination of high wave-speed and low Young's modulus and is therefore the best choice for high-speed and low actuation-voltage devices. Copper is the best choice if large actuation forces are required. For applications requiring low resistivity and low actuation voltages, Fig. 5 suggests that conductive polymers (such as doped polyaniline [47]) are attractive choices. Such polymers are not widely used in MEMS applications at present.

5. Selection of composite materials

The structures discussed thus far have been considered to be monolithic. In practice, many electrostatic actuators are composites, typically a laminate of two layers. The motivation for such structures is the ability to combine multiple functionalities with desirable structural properties. A common example is a thin metallic electrode layer (of thickness h_1) deposited on a thicker dielectric layer (of thickness h_2). The volume fractions (f) of the two materials are given by

$$f_1 = \frac{h_1}{h_1 + h_2}, \qquad f_2 = \frac{h_2}{h_1 + h_2} \tag{13}$$

where the subscripts 1 and 2 refer to the electrode and dielectric layers, respectively. The properties of the composite structure can be related to the properties of the individual components using well-established formulae. In particular, the density of the composite structure is given by [48]

$$\rho = f_1\rho_1 + f_2\rho_2 \tag{14}$$

Similarly, bounds for the values of the Young's modulus are given by [48]

$$\frac{E_1E_2}{f_1E_2 + f_2E_1} < E < f_1E_1 + f_2E_2 \tag{15}$$

As an example of the application of these relationships, consider the cantilever switch structure reported by Yao and Chang [35], which has an aluminum electrode layer of thickness 0.25 μm deposited on a silicon dioxide structural layer of thickness 2 μm. Using $\rho_{Al} = 2710$ kg/m^3, $\rho_{SiO_2} = 2200$ kg/m^3, $E_{Al} = 69$ GPa, and $E_{SiO_2} = 73$ GPa [3], it follows that the density of the composite structure is 2256 kg/m^3; the bounds for the Young's modulus converge to 72.5 GPa. These properties of the composite can then be located on the appropriate materials selection charts.

Other aspects of the selection of the components of composite structures, including the selection of contact materials [49] and dielectrics [33], have previously been addressed in the literature.

6. Conclusions

As the set of materials available to MEMS designers expands, there is a clear need for a systematic approach to the selection of materials for various applications. We have described the use of one approach, namely the Ashby methodology, for the initial selection of materials in electrostatically actuated microdevices. Performance metrics and materials indices were formulated, and materials selection charts were presented. Our analysis suggests that diamond, alumina, silicon carbide, silicon nitride, and silicon are excellent candidates for high-speed, high-force actuators; polymers for large-displacement, low actuation-voltage devices; and aluminum for low-resistivity, low actuation-voltage and high-speed actuators.

The effects of residual stresses, intrinsic damping coefficient, fatigue resistance, shock reliability, and stiction resistance on the selection of materials was discussed, along with the properties of composite structures. As the MEMS materials set expands, the coordinates of new materials can be located on the appropriate materials properties charts to determine their utility for various applications. Equally, as MEMS technologies continue to evolve, we expect that other reliability concerns will be identified (aging of polymeric structures, for example). These mechanisms will have to be included in the framework for materials selection.

References

[1] J.E. Huber, N.A. Fleck, M.F. Ashby, The selection of mechanical actuators based on performance indices, Proc. R. Soc. London, Ser. A 453 (1997) 2185–2205.

[2] S.D. Senturia, Microsystem Design, Kluwer Academic Publishers, Norwell, MA, 2001.
[3] S.M. Spearing, Materials issues in microelectromechanical systems (MEMS), Acta Mater. 48 (2000) 179–196.
[4] J.J. Sniegowski, M.P. de Boer, IC-compatible polysilicon surface micromachining, Annu. Rev. Mater. Sci. 30 (2000) 299–333.
[5] Z.J. Yao, S. Chen, S. Eshelman, D. Denniston, C. Goldsmith, Micromachined low-loss microwave switches, J. Microelectromech. Syst. 8 (1999) 129–134.
[6] H. Toshiyoshi, H. Fujita, Electrostatic microtorsion mirrors for an optical switch matrix, J. Microelectromech. Syst. 5 (1996) 231–237.
[7] P. Dubois, B. Guldimann, M.-A. Gretillat, N.F. de Rooij, Electrostatically actuated gas microvalve based on a Ta−Si−N membrane, in: Proceedings of the 14th International Conference on Micro Electro Mechanical Systems (IEEE MEMS'01), Interlaken, Switzerland, 21–25 January 2001, pp. 535–538.
[8] T.N. Pornsin-Sirirak, Y.C. Tai, H. Nassef, C.M. Ho, Flexible parylene actuator for micro adaptive flow control, in: Proceedings of the 14th International Conference on Micro Electro Mechanical Systems (IEEE MEMS'01), Interlaken, Switzerland, 21–25 January 2001, pp. 511–514.
[9] M.T.A. Saif, N.C. MacDonald, A millinewton microloading device, Sens. Actuators A 52 (1996) 65–75.
[10] H. Kahn, R. Ballarini, R.L. Mullen, A.H. Heuer, Electrostatically actuated failure of microfabricated polysilicon fracture mechanics specimens, Proc. R. Soc. London, Ser. A 455 (1999) 3807–3823.
[11] P.M. Osterberg, S.D. Senturia, M-test: a test chip for MEMS material property measurement using electrostatically actuated test structures, J. Microelectromech. Syst. 6 (1997) 107–117.
[12] B.D. Jensen, M.P. de Boer, N.D. Masters, F. Bitsie, D.A. LaVan, Interferometry of actuated microcantilevers to determine materials properties and test structure nonidealities in MEMS, J. Microelectromech. Syst. 10 (2001) 336–346.
[13] V.T. Srikar, S.M. Spearing, Microscale mechanical tests for microsystems design, Exp. Mech., 2002, in press.
[14] F. Sugihwo, M.C. Larson, J.S. Harris, Micromachined widely tunable vertical cavity laser diodes, J. Microelectromech. Syst. 7 (1998) 48–55.
[15] J. Pons-Nin, A. Rodriguez, L.M. Castaner, Voltage and pull-in time in current drive of electrostatic actuators, J. Microelectromech. Syst. 11 (2002) 196–205.
[16] E.S. Hung, S.D. Senturia, Extending the travel range of analog-tuned electrostatic actuators, J. Microelectromech. Syst. 8 (1999) 497–505.
[17] E. Quevy, P. Bigotte, D. Collard, L. Buchaillot, Large stroke actuation of continuous membrane for adaptive optics by 3D self-assembled microplates, Sens. Actuators A 95 (2002) 183–195.
[18] E.K. Chan, R.W. Dutton, Electrostatic micromechanical actuator with extended range of travel, J. Microelectromech. Syst. 9 (2000) 321–328.
[19] R. Nadal-Guardia, A. Dehe, R. Aigner, L.M. Castaner, Current drive methods to extend the range of travel of electrostatic microactuators beyond the voltage pull-in point, J. Microelectromech. Syst. 11 (2002) 255–263.
[20] J.-K. Byun, I.-H. Park, S.-Y. Hahn, Topology optimization of electrostatic actuator using design sensitivity, IEEE Trans. Magnet. 38 (2002) 1053–1056.
[21] R. Legtenberg, J. Gilbert, S.D. Senturia, M. Elwenspoek, Electrostatic curved electrode actuators, J. Microelectromech. Syst. 6 (1997) 257–265.
[22] W.C. Tang, T.-C.H. Nguyen, M.W. Judy, R.T. Howe, Electrostatic-comb drive of lateral polysilicon resonators, Sens. Actuators A21–A23 (1990) 328–331.
[23] W. Ye, S. Mukherjee, N.C. MacDonald, Optimal shape design of an electrostatic comb drive in microelectromechanical systems, J. Microelectromech. Syst. 7 (1998) 16–26.
[24] L.M. Castaner, S.D. Senturia, Speed-energy optimization of electrostatic actuators based on pull-in, J. Microelectromech. Syst. 8 (1999) 290–298.
[25] L. Castaner, A. Rodriguez, J. Pons, S.D. Senturia, Pull-in time-energy product of electrostatic actuators: comparison of experiments with simulation, Sens. Actuators A83 (2000) 263–269.
[26] M.A. Rosa, S. Dimitrijev, H.B. Harrison, Enhanced electrostatic force generation capability of angled comb finger design used in electrostatic comb drive actuators, Electron. Lett. 34 (1998) 1787–1788.
[27] H. Busta, R. Amantea, D. Furst, J.M. Chen, M. Turowski, C. Mueller, A MEMS shield structure for controlling pull-in forces and obtaining increased pull-in voltages, J. Micromech. Microeng. 11 (2001) 720–725.
[28] B. McCarthy, G.G. Adams, N.E. McGruer, D. Potter, A dynamical model, including contact bounce, of an electrostatically actuated microswitch, J. Microelectromech. Syst. 11 (2002) 276–283.
[29] R.K. Gupta, S.D. Senturia, Pull-in time dynamics as a measure of absolute pressure, in: Proceedings of the IEEE International Workshop on Microelectromechanical Systems (MEMS'97), Nagoya, Japan, 26–30 January 1997, pp. 290–294.
[30] K.Y. Yasumura, J.D. Grade, H. Jerman, Fluid damping of an electrostatic actuator for optical switching applications, in: Proceedings of the Solid-State Sensor, Actuator, and Microsystems Workshop, Hilton Head, SC, 2–6 June 2002, pp. 358–361.
[31] M.J. Kobrinsky, E.R. Deutsch, S.D. Senturia, Effect of support compliance and residual stress on the shape of doubly supported surface-micromachined beams, J. Microelectromech. Syst. 9 (2000) 361–369.
[32] V.T. Srikar, S.D. Senturia, The reliability of microelectromechanical systems in shock environments, J. Microelectromech. Syst. 11 (2002) 206–214.
[33] H.J. De Los Santos, Y.-H. Kao, A.L. Caigoy, E.D. Ditmars, Microwave and mechanical considerations in the design of MEM switches for aerospace applications, in: Proceedings of the IEEE Aerospace Conference, vol. 3, Aspen, CO, 1–8 February 1997, pp. 235–254.
[34] M.J. Madou, Fundamentals of Microfabrication, CRC Press, Boca Raton, FL, 2002.
[35] J.J. Yao, M.F. Chang, A surface micromachined miniature switch for telecommunications applications with signal frequencies from dc upto 4 GHZ, in: Proceedings of the 8th International Conference on Solid-State Sensors and Actuators (Transducers '95), Stockholm, Sweden, June 1995, pp. 384–387.
[36] P.M. Zavracky, S. Majumder, N.E. McGruer, Micromechanical switches fabricated using nickel surface micromachining, J. Microelectromech. Syst. 6 (1997) 3–9.
[37] S. Ertl, M. Adamschik, P. Schmid, P. Glauche, A. Floter, E. Kohn, Surface micromachined diamond microswitch, Diamond Relat. Mater. 9 (2000) 970–974.
[38] J.P. Sullivan, T.A. Friedman, K. Hjort, Diamond and amorphous carbon MEMS, MRS Bull. 26 (2001) 309–311.
[39] M. Mehregany, C.A. Zorman, N. Rajan, C.H. Wu, SiC MEMS for harsh environments, Proc. IEEE 86 (1998) 1594–1610.
[40] M.F. Ashby, Materials Selection in Mechanical Design, Butterworth-Heinemann, Oxford, 2001.
[41] M.F. Ashby, Multi-objective optimization in material design and selection, Acta Mater. 48 (2000) 359–369.
[42] V.T. Srikar, S.M. Spearing, Materials selection in micromechanical design: an application of the Ashby approach, J. Microelectromech. Syst., 2002, in press.
[43] K.Y. Yasumura, T.D. Stowe, E.M. Chow, T. Pfafman, T.W. Kenny, B.C. Stipe, D. Rugar, Quality factors in micron- and submicron-thick cantilevers, J. Microelectromech. Syst. 9 (2000) 117–125.
[44] V.T. Srikar, S.D. Senturia, Thermoelastic damping in fine-grained polysilicon flexural beam resonators, J. Microelectromech. Syst. 11 (2002) 499–504.
[45] C.H. Mastrangelo, Adhesion-related failure mechanisms in micromechanical devices, Tribol. Lett. 3 (1997) 223–238.
[46] C.L. Muhlstein, S.B. Brown, R.O. Ritchie, High-cycle fatigue and durability of polysilicon thin films in ambient air, Sens. Actuators A94 (2001) 177–188.

[47] A.G. MacDiarmid, Synthetic metals: a novel role for organic polymers, Synth. Met. 125 (2002) 11–22.
[48] M.F. Ashby, Criteria for selecting the components of composites, Acta Metall. Mater. 5 (1993) 1313–1335.
[49] J. Schimkat, Contact materials for microrelays, in: Proceedings of the IEEE 11th Annual International Workshop on Micro Electro Mechanical Systems (MEMS'98), Heidelberg, Germany, 25–29 January 1998, pp. 190–194.

Biographies

V.T. Srikar received the PhD degree in materials science from the Massachusetts Institute of Technology (MIT) in 1999 with a thesis on the electromigration behavior and reliability of sub-micron aluminum interconnects in silicon integrated circuits. He is currently a postdoctoral associate at MIT with research interests centered on the materials and structures issues associated with microsystems technologies. His recent research activities include the analysis of the shock reliability of MEMS, identification of a novel mode of thermoelastic damping in polysilicon microresonators, self-assembly of micro- and nano-spheres on the internal surfaces of silicon microsystems, and microscale stress measurement using Raman spectroscopy. He is involved in the fluidic packaging of the MIT microrocket device and the design and fabrication of a microfabricated solid-oxide fuel cell.

S.M. Spearing received the PhD degree from Cambridge University Engineering Department in 1990. He worked as a research engineer at the University of California at Santa Barbara from 1990 to 1992, where he produced analytical models for the failure of high-temperature ceramic materials, and at Carborundum Microelectronics, where he was a member of the electronic packaging technical development team, from 1992 to 1994. He is an associate professor of aeronautics and astronautics at the Massachusetts Institute of Technology (MIT), where he has been since 1994. His technical interests include materials and structural analysis and design of MEMS, electronic packaging and advanced composites. Since 1995, he has been responsible for the materials and structures aspects of the design and packaging of the MIT microengine, microrocket, microchemical power and microhydraulic transducer projects, as well as conducting cross-cutting underpinning technology development.